ELSEVIER

Journal of Power Sources 71 (1998) 337–347

JOURNAL OF POWER SOURCES

Effect of operating pressure on the system efficiency of a methane-fuelled solid polymer fuel cell power source

M.B.V. Virji[a,*], P.L. Adcock[a], P.J. Mitchell[a], G. Cooley[b]

[a]*Advanced Power Sources Ltd. and Loughborough University, Loughborough, Leicestershire LE11 3TU, UK*
[b]*National Power Plc., Swindon, Wiltshire, SN5 6PB, UK*

Abstract

The energy conversion efficiency of a fuel cell is directly related to its operating voltage. In general increasing the fuel and oxidant pressure increases the cell potential. However, additional energy is required to compress the gases in order to raise the pressure, negating the efficiency gains achieved in the cells. System designers seek to balance complexity, cost and system efficiency. The overall system efficiency is highly dependent on the interaction and interconnection of the components. For a system which includes a solid polymer fuel cell (SPFC) stack, a methane fuel processor and a compressor/expander an analysis has been carried out to assess the functional relationship between the operating pressure and efficiency. For a system configuration which includes a high-temperature fuel processor and a 40-kW_e stack, an 8% improvement in efficiency was predicted for the higher operating pressure (25% for 1.5 bar(a) and 33% for 4 bar(a)). © 1998 Elsevier Science S.A.

Keywords: Solid polymer fuel stack; Methane fuel; Operating pressure; System efficiency

1. Introduction

Solid polymer fuel cells (SPFCs) are becoming increasingly attractive as power sources for stationary applications. The high energy conversion efficiency and low level of noxious emissions are some of the obvious advantages the SPFC offers over conventional power sources. However, the overall system efficiency is highly dependent upon the operating condition of the individual components of the system and the choice of fuel.

A steady-state model was used to investigate the functional relationship between the operating pressure and system efficiency for a 40-kW_e SPFC system with a natural gas fuel processor. The analyses were carried out for operating pressures of 1.5 and 4 bar absolute (bar(a)). At each operating pressure the model calculates a mass and heat balance for each individual component to determine the overall electrical system efficiency. The results are presented in the form of efficiency maps, stream tables and Sankey diagrams. The maps show the electrical system efficiency as a function of compressor and expander efficiency while the stream table shows the operating conditions, energy content and gas composition in the specified stream. The Sankey diagram displays the energy flow through for the complete system.

2. SPFC system

Fig. 1 shows a schematic representation of a 40-kW_e SPFC system. The system incorporates a fuel processor, gas clean up unit (GCU), fuel cell stack and a compressor and expander. Power electronics and external heat recovery are not included.

2.1. Fuel processor

The fuel processor consists of a methane steam reformer, high-temperature shift (HTS) and low-temperature shift (LTS) reactors.

2.1.1. Methane steam reformer

The generation of hydrogen by the steam reformer requires control of thermodynamic and kinetic conditions. The critical process variables affecting the performance of the steam reformer are the steam to methane ratio, operating

* Corresponding author.

PII S0378-7753(97)02764-X

Table 1

North Sea natural gas composition

Component	Percent
CH_4	94.86
C_2H_6	3.90
i-C_4H_{10}	0.15
N_2	0.79
S (ppm)	4.0

temperature and pressure. The operating conditions chosen for use in the reformer model were a 1.5 H_2O:CH_4 molar ratio and a reformer temperature of 850°C [1–6]. Since the conversion of methane is favoured at low pressure and the formation of carbon is favoured at high pressure, the operating pressure of the reformer was analysed in the range of 1–5 bar(a) [1].

The natural gas feedstock (north sea source) has the chemical composition shown in Table 1 [4], and is first passed through a low- and high-temperature desulfurisation process whereby the majority of the sulfur is removed (0.1 ppb residual) [4]. The processed gas coming out of the desulfurisation process is assumed to be at around 350°C containing 99.2% CH_4 and 0.8% N_2. The processed gas is then fed into the reformer at two system variable pressures of 1.5 and 4 bar(a).

The reformer model was developed using the ASPEN PLUS™ software package [7]. The package calculates the percent conversion efficiency for each reactor based on thermodynamic equilibrium conditions. The percent equilibrium conversion for each reactor is calculated for a constant H_2O:CH_4 molar ratio at varying reactor temperatures. Fig. 2 shows the percent conversion versus the reformer temperature at 4 bar(a) and molar ratio of 1.5.

The operating conditions for the reformer were established to be 850°C, 4 bar(a) and a H_2O:CH_4 molar ratio of 1.5. At these conditions, the steam reformer produces 66.5, 1.6, 10.4, 18.6 and 2.7% of H_2, CH_4, H_2O, CO and CO_2 by volume, respectively. Furthermore, the CH_4 equilibrium conversion efficiency was found to be 93%. The performance of the reformer remained the same when the operating pressure was changed to the second system variable pressure of 1.5 bar(a).

2.1.2. HTS and LTS reactors

The HTS and LTS reactors were also modelled using ASPEN PLUS™. With the temperature of the HTS and LTS fixed at 400 and 150°C [4,5], respectively, the reactors were optimised to give maximum conversion of CO to H_2 by varying the H_2O:CH_4 molar ratio. The optimum ratio was found to be 0.5, which gave 70 and 77% of H_2 (vol.) from the HTS and LTS reactors, respectively. This ratio also gave 0.7% of CO from the LTS reactor.

2.2. Gas clean-up unit

The performance of SPFC is drastically reduced by the presence of CO in the fuel anode steam. The decrease in the SPFC electrochemical performance is brought about by the preferential adsorption of the CO rather than H_2 onto the platinum electrocatalytic sites on the anode. To avoid CO anode poisoning, the CO concentration in the reformed gas has to be reduced to <10 ppm (0.001%). Although there are several possible methods for removing CO from the reformed gas, the method selected for analysis here was

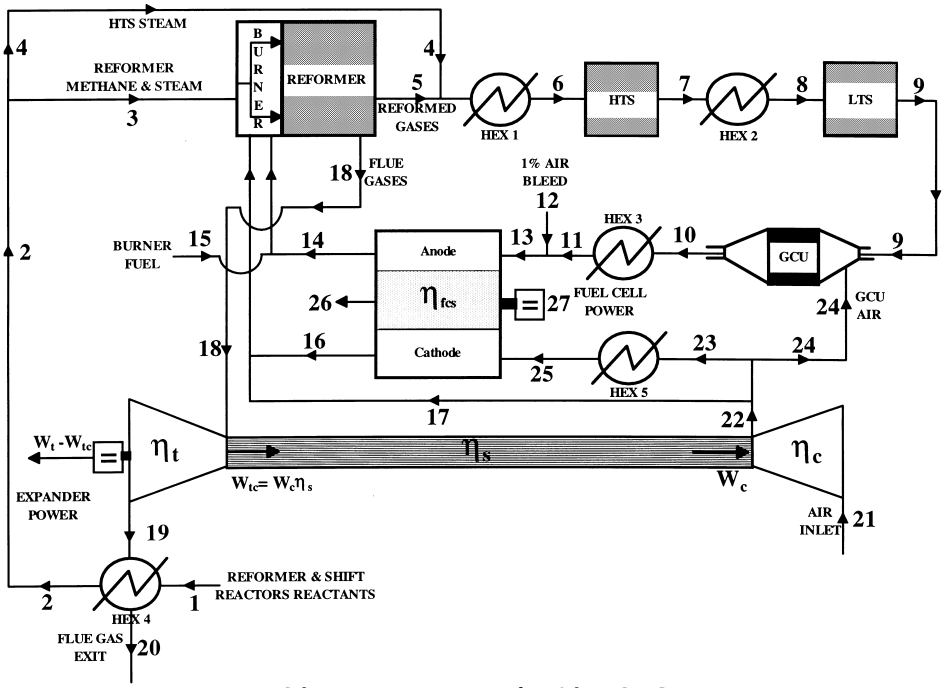

Fig. 1. Schematic representation of a 40-kW_e SPFC system.

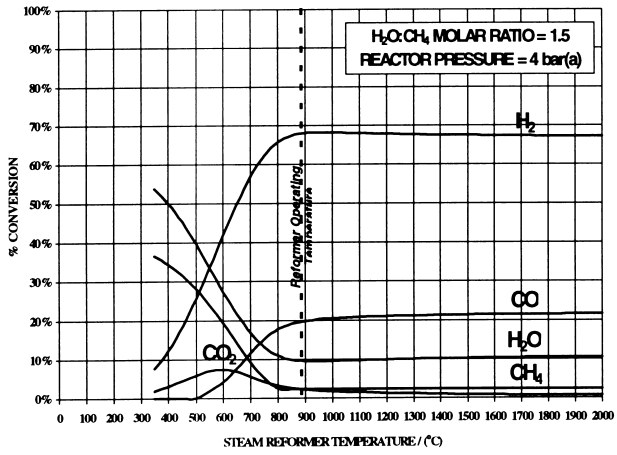

Fig. 2. Reformer equilibrium composition.

selective oxidation. The advantages of a selective oxidation reactor are fast reaction kinetics, low pressure drop and relatively low temperature operation.

The model used here incorporates the characteristics of the GCU currently being developed by the Fuel Cell Group at Loughborough University. The GCU unit, operating using a precious metal based catalyst supported on a high surface area stainless steel heat exchanger, reduces 0.7% CO in the reformate to about 5 ppm (0.0005%). An O_2:CO molar ratio of 3 was used to achieve this output level of CO.

2.3. SPFC stack

The 40-kW_e SPFC stack performance is based on a 200-cm^2 cell currently being developed by the Loughborough University Fuel Cell Group and Advanced Power Sources Ltd. Fig. 3 shows the polarisation curves for the cell on hydrogen and air at pressure of 1.5, 2 and 4 bar(a). The graph also shows the 40-kW_e power line and the operating point used in the model at a pressure of 1.5 and 4 bar(a). The cell voltage, current density and number of cells required for the two operating points are shown in Table 2.

The model uses the data shown in Table 2 to calculate the overall SPFC stack efficiency. Anode and cathode stoichiometries of 1.5 and 2, respectively, were used. A 1% air bleed, mixed with the clean reformate from the GCU, to further reduce the CO concentration, is also incorporated.

Table 2

SPFC Performance at two operating points

	Operating point	
	1	2
Air pressure (bar(a))	4.0	1.5
Cell voltage (V)	0.743	0.606
Current density (A/cm^2)	0.507	0.626
Stack power (kW_e)	40	40
Cell area (cm^2)	200	200
No. of cells	531	531
Efficiency (LHV) (%)	59	48

2.4. Compressor and expander

In this study, air provides the oxidant which is supplied at a pressure of 1.5 and 4 bar(a). The required compressor power is dependent on the flow rate, pressure ratio and isentropic efficiency [8]. The model calculates a temperature (T_2) equivalent of the compressor work for specified pressure ratio and efficiency by the following Eq. (1):

$$T_2 = \frac{T_a}{\eta_c}\left[\left(\frac{P_2}{P_a}\right)^{\left(\frac{\gamma-1}{\gamma}\right)} - 1\right] + T_a \quad (1)$$

where T_a is the air inlet temperature (K); η_c is the isentropic efficiency; P_2 is the compressor outlet pressure (bar); P_a is the compressor air inlet pressure (bar); $\gamma = 1.4$ for air.

The compressor power is supplied by the flue gas expander via a mechanical shaft with a transmission efficiency η_s of 98%. The expander power is also calculated using flue gas flow rate, pressure ratio and isentropic efficiency. The model calculates a temperature (T_4) equivalent of the expander work for specified pressure ratio and efficiency by the following Eq. (2):

$$T_4 = T_3 - \eta_t T_3\left[1 - \left(\frac{P_4}{P_3}\right)^{\left(\frac{\gamma-1}{\gamma}\right)}\right] \quad (2)$$

where T_3 is the flue gas inlet temperature (K); η_t is the isentropic efficiency; P_4 is the expander outlet pressure (bar); P_3 is the expander flue gases inlet pressure (bar); $\gamma = 1.33$ for burner flue gases.

Since the compressor and expander manufacturing efficiencies were not available, the efficiencies were varied from 0 to 100% to produce a map of efficiency versus the

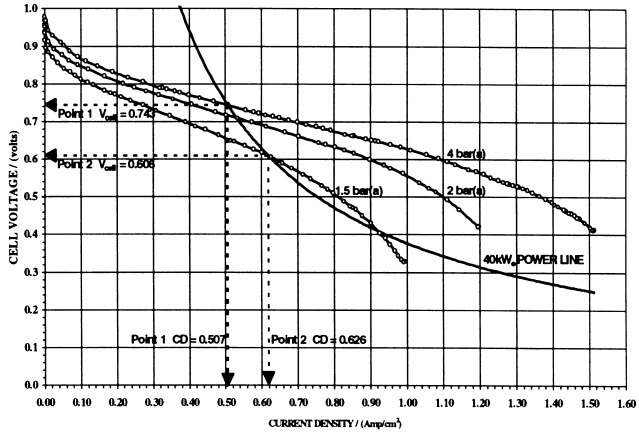

Fig. 3. Polarisation curves for a 200-cm^2 SPFC at different air pressures.

overall electrical system efficiency at two operating pressures of 1.5 and 4 bar(a).

An electrical machine was assumed to be coupled to the turbo compressor/expander shaft to balance the compressor/expander power. This would also enable system pressurisation during start up.

3. Steady-state system calculations

Two system operating pressures of 1.5 and 4 bar(a) were modelled. The system was based on a net fuel cell output of 40 kW_e. The model employed the data and the operating conditions described in the previous section.

3.1. Mass and energy balances

The law of conservation of mass states that in any process, mass is neither created nor destroyed; thus

(mass in) = (mass out)

+ (accumulation or depletion within the system)

Similarly, energy is conserved in any plant or unit, though the additional complication of conversion between forms of energy may be important [9,10]. The following principles of mass and heat balance were used to performance the calculation in this section. The mass balance assumed that the flow rate is the same throughout a unit or component of the system. The heat balance involved calculating the specify heat capacity C_p and calorific value (LHV) of individual gases as function of temperature. The heat balance was based on net calorific value or LHV of the fuel. The dew point temperature was also determined for each gas stream. The dew point, determined by the partial pressure of the vapour in a gas stream, was used to calculate the energy of the water vapour in the saturated stream. The energy associated with the compression and expansion of the gases was also taken into account.

3.2. System assumptions

A number of other assumptions for the system based on typical reported data have been made as detailed below.

1. All calculations were made relative to a datum temperature of 25°C.
2. The pressure drop over the various components of the system can be neglected.
3. The energy used in the desulfurisation process is not accounted for.
4. The reformer processed gas feed is 99.2% CH_4, 0.8% N_2 and at a temperature of 350°C.
5. Two percent reformer surface losses [5].
6. The reformer, HTS and LTS reactors exit streams are at equilibrium.
7. Electrical requirement for all the ancillary equipment was not considered.
8. All heat exchangers are assumed to have 0.8 effectiveness.
9. Methane in the reformed gas from the reformer is not consumed in the HTS, LTS, GCU and SPFC.
10. All CO is oxidised by the 1% air bleed with the rest of the oxygen oxidising H_2.
11. 10% excess air is used in the burner and the burner efficiency is assumed to be 100%.

3.3. SPFC stack

The SPFC stack operating at a temperature of 80°C, pressures of 1.5 and 4 bar(a) utilises 65% of the hydrogen. The total clean reformate required at this hydrogen utilisation is 1071 and 868 SLPM, respectively. The air required by the stack at cathode stoichiometry of 2 is 2205 and 1787 SLPM, respectively. The theoretical thermal fuel cell efficiency η_{fc} (LHV) is given by

$$\eta_{fc} = \Delta_r G / \Delta_r H$$

where

$\Delta_r G$ is the free energy available in H_2;

$\Delta_r H$ is the heat of combustion of H_2

Also, maximum heat out of the fuel is given by the difference of $\Delta_r H - \Delta_r G$. The η_{fc} (LHV) calculated for the two operating pressures of 1.5 and 4 bar(a) are 48% and 59%, respectively. The energy balances of the stack at the two operating pressures is shown in Table 3.

To maintain the fuel cell stack at 80°C the heat to be removed by the cooling system is 27.6 and 15.2 kW at the two operating pressures of 1.5 and 4 bar(a), respectively.

3.4. Fuel processor

3.4.1. Reformer reactants

The processed natural gas feed rates for the 40-kW_e SPFC power at the two operating pressures of 1.5 and 4 bar(a) were calculated to be 198 and 160 SLPM. The corresponding energy in the feed at 298°C, including the steam, is found to 132 and 107 kW.

3.4.2. Reformer reactions

Hydrogen is produced in a steam reformer by reacting methane with steam over a supported nickel catalyst at temperature of 850°C [1–6]. In the reaction the methane is converted into hydrogen and carbon monoxide

$$CH_4 + H_2O \leftrightarrow CO + 3H_2 \quad \Delta H_{1123\ K} = 22.99\ kJ/mol$$

The CO reacts further via the water shift reaction to produce more H_2 and CO_2

Table 3

SPFC Stack energy balance

	Operating pressure							
	15 Bar(a)				4 Bar(a)			
	Energy into the stack (kW)	Energy into the stack (%)	Energy out of the stack (kW)	Energy out of the stack (%)	Energy into the stack (kW)	Energy into the stack (%)	Energy out of the stack (kW)	Energy out of the stack (%)
Anode inlet	134.6	98.1			109.1	98.0		
Cathode air	2.5	1.9			22	2.0		
Stack power			40.3	29.4			40.0	36.0
Anode exhaust			51.1	37.3			41.4	37.2
Cathode exhaust			18.1	13.2			14.7	13.2
Cooling system			27.6	20.1			15.2	13.6
Total	137.1	100	137.1	100	111.3	100	111.3	100

$$CO + H_2O \leftrightarrow CO_2 + H_2 \quad \Delta H_{1123\,K} = -33.47\ \mathrm{kJ/mol}$$

When calculating the heat of reformation, the above reactions are considered. There are other reactions which are responsible for production of H_2, but when dealing with equilibrium relationships these equations are not considered important. However, when dealing with the kinetic relationships then the choice of equations is significant [2]. The heat of reformation calculated for each operating point using the two equations is found to be 31 and 25 kW, respectively.

3.4.3. Reformed gases

The reformer equilibrium conversion efficiency is found to be 93%. At this efficiency the reformed gas consists of following proportions of gases (vol.%):

H_2	66.50%
CO	18.60%
CO_2	2.70%
H_2O	10.40%
N_2	0.20%
CH_4	1.60%

Total energies in the reformed gases at 850°C and pressures of 1.5 and 4 bar(a) are 155 and 125 kW, respectively.

3.4.4. Reformer burner

The burner is supplied with the fuel cell stack exhaust gases, processed natural gas and air from the compressor. The amount of supplementary processed natural gas supplied to the burner is determined by performing a heat balance on the reformer and maintaining the reformer's temperature at 850°C; 10% excess air is also supplied to ensure complete combustion. Table 4 shows the reformer heat balance and the amount of extra energy required from the processed natural gas. The extra energy corresponds to 75 and 57 SLPM of processed natural gas at operating points 1 and 2, respectively. The fuel gases from the burner are supplied to an expander at the reformer temperature.

The overall reformer efficiency η_r given by the energy in reformed gases as fraction of the total energy in the reformer is shown in the table to be approximately 58%.

3.5. HTS and LTS reactors

HTS and LTS reactors are assumed to be heated to the operating temperature by the reformed gases. Only the inlet and outlet conditions of the reactants and products are considered for the heat and mass balance. The only reaction considered in the shift reactors is the water shift reaction. CO from the reformer is reduced from 18.6% to 7.3% in the HTS and subsequently reduced to 0.7% in the LTS reactor. The reformate gas composition from the outlet of the HTS and LTS reactors is shown below (vol.%):

	HTS	LTS
H_2	70.10%	76.70%
CO	7.30%	0.70%
CO_2	12.00%	18.70%
H_2O	9.40%	2.70%
N_2	0.20%	0.20%
CH_4	1.00%	1.00%

To maintain the HTS and LTS reactors at an operating temperature of 400 and 200°C, respectively, the heat to be removed by the cooling system is 5 and 4 kW at a pressure of 1.5 bar(a) and 4 and 3 kW at a pressure of 4 bar(a) for HTS and LTS reactors, respectively.

3.6. GCU reactor

The GCU reactor preferentially oxidises the CO to CO_2 over a heterogeneous catalyst at a temperature of about 150°C.

$$CO + 1/2\ O_2 \leftrightarrow CO_2 \quad \Delta H_{423\ K} = -283.49\ kJ/mol$$

At the operating conditions detailed in Section 2.2, CO is reduced to 5 ppm and the heat energy removed from the GCU to maintain a temperature of 150°C is calculated to be 6.2 and 5.3 kW at the two operating pressures. This heat energy also contains hydrogen energy from its reaction with the excess oxygen. The clean reformate form the GCU reactor has the following gas composition:

CO	0.0005%
CH_4	0.93%
H_2	67.84%
CO_2	17.98%
H_2O	5.75%
N_2	7.51%

3.7. Air bleed (1%)

To further reduce the CO concentration in the clean reformate from the GCU reactor, 1% air bleed is mixed with reformate prior to the fuel cell anode inlet. It was assumed that the CO was completely burnt and all excess oxygen reacts with hydrogen rather than methane. About 2% of the hydrogen energy was lost as heat by the chemical reaction.

3.8. Heat exchangers

Heat and mass balance for all the heat exchangers was performed by considering only the inlet and outlet conditions of the gas streams. Table 5 shows the heat energy out of each heat exchanger at the two operating points.

From Table 5 it can be seen that heat exchanger number five is not required for the system pressure of 1.5 bar(a), since the air temperature out of the compressor is below 80°C.

3.9. Compressor and expander

The efficiency of the compressor and expander has been taken as 70%. However, in order to understand the effect of compressor and expander system over the overall electrical system efficiency, the compressor and expander isentropic efficiencies are varied from 0 to 100%.

At 70% compressor efficiency, the air temperature at the outlet of the compressor, at a pressure ratio of 1.5 is calculated to be 77°C while for pressure ratio of 4 the temperature is calculated to be 232°C. The corresponding compressor power is determined to be 3.1 and 10.2 kW for respective pressure ratios of 1.5 and 4. Including the mechanical transmission efficiency of the shaft (η_s = 98%), the total power required by the compressor at pressure ratio of 1.5 and 4 is 3.2 and 10.4 kW, respectively.

Expander power is also calculated, using Eq. (2) in Section 2.4, for pressure ratios of 1.5 and 4. The flue gases at the temperature of 850°C are expanded to the temperatures of 774 and 620°C at the pressure ratios of 1.5 and 4, respec-

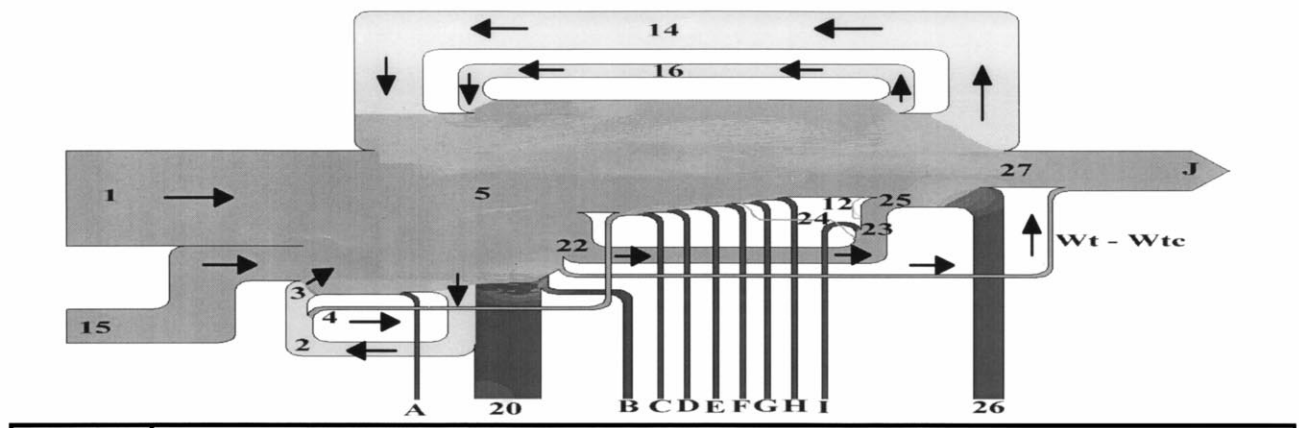

	1	2	3	4	5	12	14	15	16	20	23	24	25	26	27
1.5 bar(a) kW	132	17	13	4	155	0.04	51	50	18	80	3	0.11	3	28	40
1.5 bar(a) %	73%	9%	7%	2%	85%	0.02%	28%	27%	10%	44%	1%	0.1%	1%	15%	22%
4.0 bar(a) kW	107	14	10	3	125	0.02	41	39	15	51	9	0.37	2	15	40
4.0 bar(a) %	73%	9%	7%	2%	86%	0.02%	28%	27%	10%	35%	6%	0.3%	2%	10%	27%

	A	B	C	D	E	F	G	H	I	J		NOTES	
	Reformer	HEX 4	HEX 1	HTS	HEX 2	LTS	GCU	HEX 3	HEX 5	ELECTRIC POWER	Wt -Wtc	Letters - Energy Out of the System Numbers - Refer to numbers on System Diagram	
1.5 bar(a) kW	5	3	3	5	3	4	6	1	0	45	5		
1.5 bar(a) %	3%	2%	2%	3%	2%	2%	3%	1%	0%	25%	3%		
4.0 bar(a) kW	4	3	2	4	2	3	5	1	6	48	8	Compressor Efficiency	70%
4.0 bar(a) %	3%	2%	2%	3%	2%	2%	4%	1%	4%	33%	6%	Expander Efficiency	70%

Fig. 4. Sankey diagram for both operating pressures of 1.5 and 4 bar(a).

Table 4

Reformer energy balance

	Operating pressure							
	15 Bar(a)				4 Bar(a)			
	Energy into the reformer (kW)	Energy into the reformer (%)	Energy out of the reformer (kW)	Energy out of the reformer (%)	Energy into the reformer (kW)	Energy into the reformer (%)	Energy out of the reformer (kW)	Energy out of the reformer (%)
Reformer reactants	148.6	55.5			120.4	56.0		
Burner reactants	119.1	44.5			94.8	44.0		
Burner flue gases			10.7	40.2			85.7	39.8
Reformed gases			154.7	57.8			125.3	58.2
Surface losses			5.2	2.0			4.2	2.0
Total	267.7	100	267.7	100	215.2	100	215.2	100

tively. The power generated by the expander at isentropic efficiency of 70% is 7.9 and 18.6 kW at pressure ratios of 1.5 and 4, respectively. Extra power from the expander can be combined with fuel cell stack power and supplied to the system load.

4. Results

4.1. Sankey diagram

The Sankey diagram shown in Fig. 4 shows the energy flow through the system. From this diagram it can be seen that the percentage of the heating value of the processed natural gas converted to useful electrical power is 25 and 33% for a system operating on pressure of 1.5 and 4 bar(a), respectively.

With compressor and expander efficiencies of 70%, the electric power contribution from the expander is 3 and 6% at the two operating pressure of 1.5 and 4 bar(a), respectively. Furthermore, it can also be seen for both the operating pressures that the largest energy loss in the system is due to the flue gases. However, some of this energy can be further recovered by a waste heat boiler and economizer [8,9].

4.2. Stream tables

Tables 6 and 7 show the stream tables for the two operating pressures of 1.5 and 4 bar(a), respectively. The stream numbers correspond to those seen in Fig. 1. At each stream number the table shows the following properties of stream:

1. temperature (K)
2. pressure (bar(a))
3. molar flow rate (mol/s)
4. volume flow rate (SLPM)
5. energy content (kW)
6. total energy into the system (%)
7. gas composition (%)

4.3. Electrical system efficiency as a function of compressor and expander efficiencies.

Figs. 5 and 6 show efficiency maps for operating pressures of 1.5 and 4 bar(a). The electrical efficiency is the fraction of total electrical power in the system divided by the total heating value of the processed natural gas (LHV). The total electrical power is calculated by taking the fuel cell power and adding the net difference between the expander and compressor power multiplied by 0.9 (electrical machine efficiency).

5. Discussion and conclusions

Referring to Figs. 1 and 4, it is evident that large amounts of energy are re-circulated within the SPFC system. The fuel cell anode and cathode exit gases (14 and 16) represent energy flows of 51 and 18 kW, respectively, for the 1.5 bar(a) case and 41 and 15 kW for the 4 bar(a) case. This includes the chemical, thermal and compressed gas energies. The larger values for the low pressure case are due to the increased flow rates of reactants required for the increased current from the cells (101–125 A) while maintaining the stoichiometry at 1.5 for the anode and 2.0 for the cathode.

Table 5

Heat energy out of the heat exchangers

	Heat energy out (kW)	
	1.5 Bar(a)	4 Bar(a)
HEX1	3.0	2.4
HEX2	2.9	3.2
HEX3	1.0	0.8
HEX4	3.3	2.7
HEX5	0.0	6.3
Total	10.2	15.5

Table 6

Stream table for operating pressure of 1.5 bar(a)

	1 Reformer and shift reactor reactants	2 Preheated reactants	3 Reformer preheated reactants	4 Shift reactor preheated reactants	5 Reformer reformed gas	6 HEX1 outlet	7 HTS reactor outlet	8 HEX2 outlet	9 LTS reactor outlet	10 GCU reactor outlet	11 HEX3 outlet	12 Air bleed	13 Anode inlet	14 Anode exhaust
Temperature (K)	298	623	623	623	1123	673	673	423	423	423	353	353	353	353
Pressure (bar(a))	1.5	1.5	1.5	1.5	1.5	1.5	1.5	1.5	1.5	1.5	1.5	1. 5	1.5	1.5
Molar flowrate (mol/s)	0.44	0.44	0.37	0.07	0.64	0.71	0.72	0.72	0.72	0.78	0.78	0.03	0.80	0.45
Volume flowrate (SLPM)	596	596	497	99	861	960	968	968	968	1045	1045	34	1071	608
Energy (kW)	132	149	145	4	155	156	151	148	144	138	137	0.04	135	51
Total energy (%) (1 + 15)	73	82	79	2	85	86	83	81	79	76	75	0. 02	74	28
Composition (%)														
H_2	–	–	–	–	67	60	70	70	77	68	68	–	65	38
CO	–	–	–	–	19	17	7	7	1	5 ppm	5 ppm	–	0	0
CO_2	–	–	–	–	3	2	12	12	19	18	18	–	18	31
H_2O	57	57	50	7	10	20	9	9	3	6	6	–	7	12
N_2	0.27	0.27	0.27	–	0.20	0.18	0.20	0.20	0.20	8	8	79	10	17
CH_4	33	33	33	–	2	1	1	1	1	1	1	–	1	2
O_2	–	–	–	–	–	–	–	–	–	0	0	21	0	–

	15 Burner fuel	16 Cathode exhaust	17 Burner air	18 Burner flue gases	19 Expander flue gases outlet	20 HEX4 outlet	21 Compressor air inlet	22 Compressor air outlet W_{ts}	23 Fuel cell air and bleed air	24 GCU air	25 Hex5 outlet	26 Fuel cell system cooling	27 Fuel cell electrical power	28 Expander electrical power $W_{t-}W_{tc}$
Temperature (K)	623	353	350	1123	1047	852	298	350	350	350	350	353	353	1123
Pressure (bar(a))	1.5	1.5	1.5	1.5	1.0	1.0	1.0	1.5	1.5	1.5	1.5	1.5	1.5	1.5
Molar flowrate (mol/s)	0.06	1.81	0.30	2.54	2.54	2.54	2.04	2.04	1.64	0.07	1.64	–	–	–
Volume flowrate (SLPM)	75	2437	403	3408	3408	3408	2739	2739	2205	97	2205	–	–	–
Energy (kW)	50	18	0.5	108	100	80	0	3	3	0.11	3	28	40	5
Total energy (%) (1 + 15)	27	10	0	59	55	44	0	2	1	0.1	1	15	22	3
Composition (%)														
H_2	–	–	–	0	0	0	–	–	–	–	–	–	–	–
CO	–	–	–	0	0	0	–	–	–	–	–	–	–	–
CO_2	–	–	–	8	8	8	–	–	–	–	–	–	–	–
H_2O	–	19	–	28	28	28	–	–	–	–	–	–	–	–
N_2	–	71	79	64	64	64	79	79	79	79	79	–	–	–
CH_4	100	–	–	0	0	0	–	–	–	–	–	–	–	–
O_2	–	10	21	1	1	1	21	21	21	21	21	–	–	–

Table 7

Stream table for operating pressure of 4 bar(a)

	1 Reformer and shift reactor reactants	2 Preheated reactants	3 Reformer preheated reactants	4 Shift reactor preheated reactants	5 Reformer reformed gas	6 HEX1 outlet	7 HTS reactor outlet	8 HEX2 outlet	9 LTS reactor outlet	10 GCU reactor outlet	11 HEX3 outlet	12 AIR bleed	13 Anode inlet	14 Anode exhaust
Temperature (K)	298	623	623	623	1123	673	673	423	423	423	353	353	353	353
Pressure (bar(a))	4	4	4	4	4	4	4	4	4	4	4	4	4	4
Molar flowrate (mol/s)	0.36	0.36	0.30	0.06	0.52	0.58	0.58	0.58	0.58	0.63	0.63	0.02	0.6458	0.367
Volume flow rate (SLPM)	483	483	403	80	698	778	784	784	784	846	846	27	868	493
Energy (kW)	107	120	117	3	125	126	122	120	117	112	111	0.03	109	41
Total energy (%) (1 + 15)	73	83	80	2	86	87	84	82	80	77	76	0.02	75	28
Composition (%)														
H_2	–	–	–	–	67	60	70	70	77	68	68	–	65	38
CO	–	–	–	–	19	17	7	7	1	5 ppm	5 ppm	–	0	0
CO_2	–	–	–	–	3	2	12	12	19	18	18	–	18	31
H_2O	52	52	50	2	10	20	9	9	3	6	6	–	7	12
N_2	0.27	0.27	0.27	–	0 20	0.18	0.20	0.20	0 20	8	8	79	10	17
CH_4	33	33	33	–	2	1	1	1	1	1	1	–	1	2
O_2	–	–	–	–	–	–	–	–	–	0	0	21	0	–

	15 Burner fuel	16 Cathode exhaust	17 Burner air	18 Burner flue gas	19 Expander flue gases outlet	20 HEX4 outlet	21 Compressor air inlet	22 Compressor air outlet W_{ts}	23 Fuel cell air and bleed air	24 GCU air	25 HEX5 outlet	26 Fuel cell system cooling	27 Fuel cell electrical power	28 Expanded electrical power $W_{t-}W_{tc}$
Temperature (K)	623	353	505	1123	893	682	298	505	505	505	353	353	353	1123
Pressure (bar (a))	4	4	4	4	1	1	1	4	4	4	4	4	4	4
Molar flowrate (mol/s)	0.04	1.47	0.21	2.01	2.01	2.01	1.61	1.61	1.33	0.06	1.33	–	–	–
Volume flowrate (SLPM)	57	1974	276	2707	2707	2707	2169	2169	1787	78	1787	–	–	–
Energy (kW)	39	15	1	86	67	51	0	10	9	0.37	2	15	40	8
Total energy (%) (1 + 15)	27	10	1	59	46	35	0	7	6	0.3	2	10	27	6
Composition (%)														
H_2	–	–	–	0	0	0	–	–	–	–	–	–	–	–
CO	–	–	–	0	0	0	–	–	–	–	–	–	–	–
CO_2	–	–	–	8	8	8	–	–	–	–	–	–	–	–
H_2O	–	19	–	28	28	28	–	–	–	–	–	–	–	–
N_2	–	71	79	63	63	63	79	79	79	79	79	–	–	–
CH_4	100	–	–	0	0	0	–	–	–	–	–	–	–	–
O_2	–	10	21	1	1	1	21	21	21	21	21	–	–	–

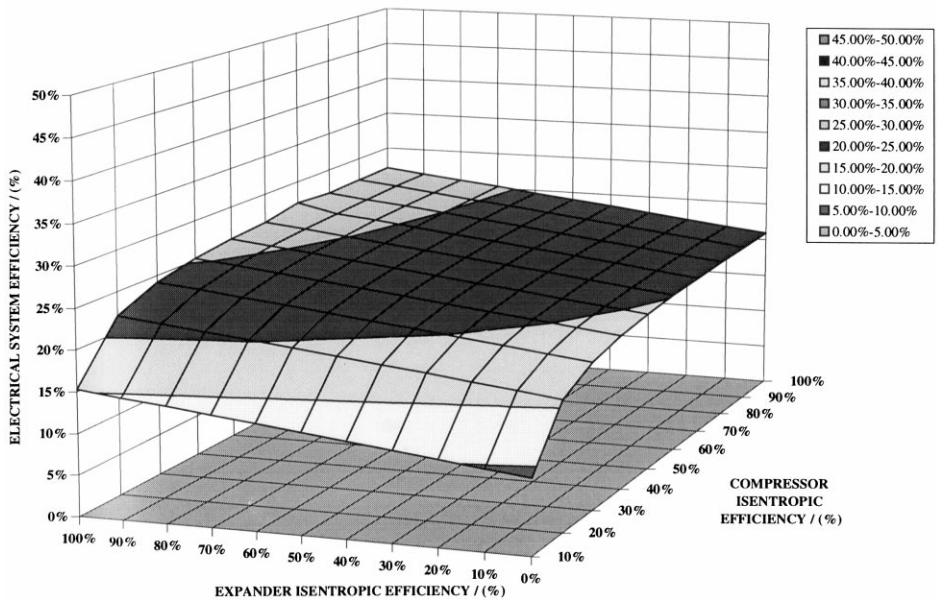

Fig. 5. Efficiency map for operating pressure of 1.5 bar(a).

Energy is recovered from the flue gas by the expander (18–19) and heat exchanger 4 (19–20). Excess energy flowing from the turbo expander (5 and 8 kJ/s) is recovered by a small high-speed electrical machine. Further energy could be recovered for external use from the thermal losses; however, this has not been included in this study.

Table 8 shows the approximate efficiencies of the main components in the system. Each efficiency is defined as following:

$$\eta_{\mathrm{R}} = \frac{\text{Net electric energy generated in expander}^{+}}{\text{Heating value of processed NG to reformer}^{*}}$$

$$\eta_{\mathrm{FCS}} = \frac{\text{Electric energy generated in fuel cell stack}}{\text{Heating value of processed NG to reformer}^{*}}$$

* Also includes the processed gas to reformer burner

$^{+}$ Expander power − (Compressor power + shaft power loss)

The overall system efficiencies (η_{total}) from fuel energy (LHV) to electrical energy were predicted to be 25% for the 1.5 bar(a) system and 33% for the 4 bar(a) system. As with any modelling exercise, the validity of the predictions are

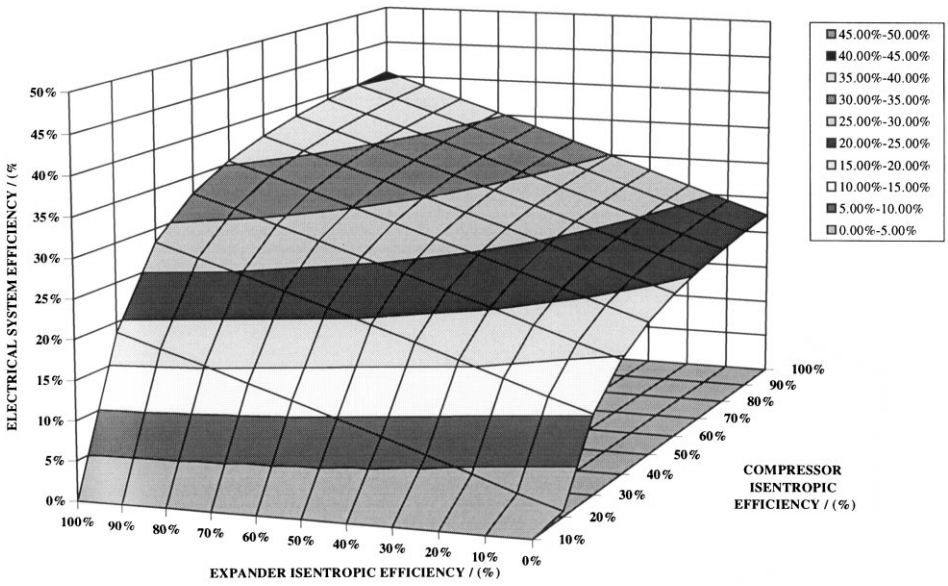

Fig. 6. Efficiency map for operating pressure of 4 bar(a).

Table 8

Efficiencies at the two operating pressures

	Operating pressure	
	1.5 Bar(a)	4 Bar(a)
η_R (%)	3	6
η_{FCS} (%)	22	28
η_{total} (%)	25	33

dependent on how well the mathematical models fit the real components. For the case of the turbo compressor/expander, an isentropic efficiency of 70% was assumed for each part. For such a small machine this may be optimistic, therefore curves have been included which relate their efficiency to the overall system efficiency, excluding the electrical energy recovery from the shaft generator (Figs. 5 and 6). From these it is immediately apparent that the system efficiency for the high pressure case is extremely dependent upon the performance of the turbo machine, whereas for the case of the low pressure system the flatter shape indicates that the efficiency is much less dependant on the turbo compressor/expander.

Improved thermal integration and heat transfers for the heat exchangers coupled with more selective catalysts for the GCU and improved CO tolerant anode electrodes should lead to system efficiencies of between 35 and 40%.

The principal advantage of operating at 1.5 bar(a) as opposed to 4 bar(a) is that the turbo machinery is less complex and less expensive. However, the stack efficiency, η_{FCS}, is reduced and more energy is lost from the flue. If there were no expander in the system (expander efficiency = 0%) then the efficiency of both high and low pressure systems would be 20%.

For the system configuration which includes a high-temperature fuel processor and a 40-kW_e stack, an 8% improvement in efficiency was predicted for the higher operating pressure (25% for 1.5 bar(a) and 33% for 4 bar(a), fuel to electrical energy).

The higher pressure system efficiency is highly dependent upon the performance of the turbo compressor/expander. For example, if the compressor and expander were 80 rather than 70% efficient, then the high-pressure system efficiency would be 36% and the low-pressure system would be 26%.

References

[1] E.S. Wagner and F. Froment, *Hydrogen Processing, July* (1992) 69.
[2] M.H. Hyman, *Hydrogen Processing, July* (1968) 131.
[3] W. W. Akers and D. Camp, *A.I.Ch.E J., 1(4)* (1955) 471.
[4] A. Dicks, *J. Power Sources, 61* (1995) 113.
[5] S. Elnashaie and S. Elshishini, *Modelling, Simulation and Optimisation of Industrial Fixed Bed Catalytic Reactors*, Topics in Chemical Engineering, Vol. 7, 1993.
[6] L. Blomen and M. Mugerwa, *Fuel Cell Systems*, Plenum, New York and London, 1993.
[7] ASPEN PLUS™ (chemical engineering modelling software package), Aspen Technology Inc. (Aspen Tech), Release 9.3–1, September 1996, 10 Canal Park, Cambridge, MA.
[8] H. Cohen, G. Rogers and H. Saravanamuttoo, *Gas Turbine Theory*, 2nd Edition, Longman, England, 1972.
[9] J. Harker and J. Backhurst, *Fuel and Energy*, Academic, London, 1981.
[10] T. Eastop and D. Croft, *Energy Efficiency (for Engineers and Technologists)*, Longman, New York, 1990.